Journal of Power Sources 195 (2010) 4676–4684

Contents lists available at ScienceDirect

Journal of Power Sources

journal homepage: www.elsevier.com/locate/jpowsour

Crosslinked membranes of sulfonated polyimides for polymer electrolyte fuel cell applications

Kazuaki Yaguchi, Kangcheng Chen, Nobutaka Endo, Mitsuru Higa, Ken-ichi Okamoto*

Graduate School of Science & Engineering, Yamaguchi University, Tokiwadai 2-16-1, Ube, Yamaguchi, 755-8611, Japan

ARTICLE INFO

Article history:
Received 12 November 2009
Accepted 30 January 2010
Available online 6 February 2010

Keywords:
Polymer electrolyte fuel cell
Crosslinked sulfonated polyimide
Hydrogen crossover
Back-diffusion of water
Polymer electrolyte membrane

ABSTRACT

Polymer electrolyte fuel cell performance of crosslinked membranes of sulfonated polyimides based on 2,2′-bis(3-sulfophenoxy) benzidine was investigated at higher temperatures of 90–110 °C, relative humidities of 82–27% RH and pressures of 0.3–0.1 MPa. The operation conditions of temperature, pressure and relative humidity largely affected the PEFC performance in connection with each other. At 90 °C and relatively high humidification of 82/68% RH for hydrogen/air, the cell performance was hardly affected by the pressure and was kept in a high level even at 0.1 MPa. At low humidification of 48% and 27% RH, the cell performance was still kept in a reasonably high level at high pressures above 0.2 MPa, but it largely decreased at low pressures below 0.15 MPa. A slight decrease in ion exchange capacity (IEC) of membrane caused a relatively large decrease in the cell performance at a low relative humidity. With an increase in temperature from 90 to 110 °C, the cell performance largely decreased. For example, the membrane (MX2) with a relatively high IEC of 1.9 mequiv g^{-1} showed a low maximum output (W_{max}) of 0.30 W cm^{-2} at 110 °C, 0.2 MPa and 49% RH, which was less than a half of the corresponding value (0.71 W cm^{-2}) at 90 °C. These results indicate that the back-diffusion of water formed at cathode into membrane became less effective at the lower pressure and the higher temperature and for membrane with the lower IEC, resulting in the larger decrease in *through-plane* proton conductivity under PEFC operation. At 110 °C, 0.3 MPa and 49% RH, MX2 showed the fairly high PEFC performance and durability.

1. Introduction

Polymer electrolyte fuel cells (PEFCs) have been attracting great attention as clean energy sources of residential cogeneration, vehicular transportation and other applications. Polymer electrolyte membrane (PEM) is a key component playing a critical role on PEFC performance. Perfluorosulfonic acid polymer membranes such as Nafion (DuPont) are state-of-the-art membranes because of their high proton conductivity and excellent chemical stability [1–3]. However, they have some disadvantages such as low operational temperatures below 80 °C and high fuel gas and oxygen crossover. Much research has been done to develop alternative PEMs based on sulfonated aromatic polymers [1,3–23]. Generally, the aromatic PEMs have some shortcomings such as relatively low proton conductivity at low relative humidities and relatively low membrane stability in PEFC operation.

To improve both the cell efficiency and feasibility, it is desirable to operate PEFCs at high temperatures above 100 °C and low relative humidities below 50% [7,12,18]. Recently we reported on side-chain-type sulfonated polyimides (SPIs) derived from 1,4,5,8-naphthalene tetracarboxylic dianhydride (NTDA) and 2,2′-bis(3-sulfophenoxy) benzidine (BSPOB) and their SO_2-crosslinked membranes [21,24,25]. They showed high performance and durability for PEFCs operated at 90 °C and 0.3 MPa (H_2/air) in wide humidity range of 84–30% RH [22]. The reasonably high PEFC performance at 30% RH was attributed to the effective back-diffusion of water molecules formed at the cathode. In this paper, we report on the PEFC performances of crosslinked SPI membranes with different ion exchange capacities at higher temperatures of 90–110 °C and in wide ranges of pressure (0.3–0.1 MPa) and relative humidity (82–27% RH).

2. Experimental

2.1. Preparation of crosslinked SPI membranes

The random copolyimides were prepared from NTDA, BSPOB and 1,3-bis(4-aminophenoxy) benzene (BAPBz) according to the reported method [21]. The SPIs prepared were NTDA-BSPOB/BAPBz(2/1) and NTDA-BSPOB/BAPBz(3/1) where the data in parentheses refer to the molar ratio of BSPOB to BAPBz.

* Corresponding author. Tel.: +81 836 85 9660; fax: +81 836 85 9601.
E-mail address: okamotok@yamaguchi-u.ac.jp (K.-i. Okamoto).

0378-7753/$ – see front matter © 2010 Elsevier B.V. All rights reserved.
doi:10.1016/j.jpowsour.2010.01.081

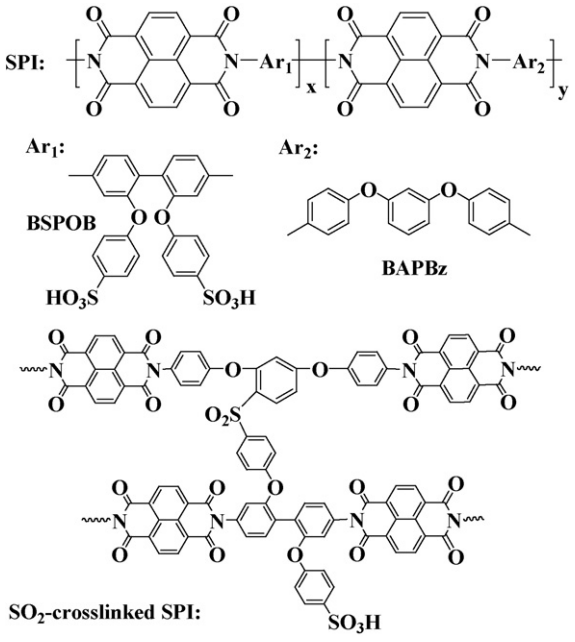

Fig. 1. Chemical structure of SPI and SO_2-crosslinked SPI membranes.

SPI membranes were prepared by casting their 5–6 wt% *m*-cresol solutions (in triethylamine (TEA) form) onto glass plates, followed by residue extraction in methanol, proton exchange and curing [21]. The dry SPI membranes were immersed in a solution of phosphorous pentoxide and methane sulfonic acid (PPMA) (1/10 in weight ratio) at 30 °C for 48 h to form SO_2-crosslinking [22,24,25]. The crosslinked membranes were thoroughly washed with ultrapure water and then dried in vacuum. The chemical structures of SPI and crosslinked one are shown in Fig. 1.

2.2. Membrane characterization

Ion exchange capacity (IEC) was evaluated by a titration method. Water uptake and dimensional change of membrane were measured according to the methods described elsewhere [18,19]. Water uptake (*WU*) was calculated from Eq. (1):

$$WU = \frac{W_s - W_d}{W_d} \times 100\% \quad (1)$$

where W_d and W_s are the weights of dry and corresponding water-swollen membranes, respectively. Dimensional changes in thickness (Δt_c) and in plane direction (Δl_c) were calculated from Eq. (2):

$$\Delta t_c = \frac{t - t_d}{t_d}$$

$$\Delta l_c = \frac{l - l_d}{l_d} \quad (2)$$

where t_d and l_d are the thickness and length of the dry membrane, respectively; t and l refer to those of the membrane swollen in water.

In-plane and *through-plane* proton conductivities ($\sigma_{//}$and $\sigma_{\perp}$, respectively) of SPI membrane were determined using an electrochemical impedance spectroscopy technique over the frequency from 100 Hz to 100 KHz (Hioki 3532-80). The cell was placed under either in a thermo-controlled humidic chamber or in liquid water [21]. For $\sigma_{\perp}$, a membrane sample was set between two platinum plate electrodes of 1 cm^2 area, and mounted on two Teflon blocks [23]. The cell was placed in liquid water. Proton conductivity ($\sigma_{//}$ and $\sigma_{\perp}$) was calculated from Eq. (3):

$$\sigma_{//} = \frac{d}{t_s w_s R}$$

$$\sigma_{\perp} = \frac{t_s}{AR} \quad (3)$$

where d is the distance between the two electrodes, t_s and w_s are the thickness and width of the membrane at a standard condition of 70% RH, respectively, A is the electrode area, and R is the resistance value measured. The thickness of a water-swollen membrane was used in the calculation of both $\sigma_{//}$and $\sigma_{\perp}$ in the fully hydrated state.

2.3. Fabrication of membrane electrode assembly (MEA) and measurements of cell performance

An MEA was fabricated from a membrane sample by hot-pressing an electrode/membrane/electrode sandwich at 150 °C for 5 min under 60 kgf cm^{-2}. Prior to the hot-pressing, both surfaces of the membrane and Pt/C electrodes (Johnson Matthey Plc., #45372) were impregnated with a small amount of Nafion solution as a binder. The effective electrode area was 5 cm^2. The MEA was set in a single cell test fixture and mounted in to an in-house fuel cell test station (NF Inc., model As-510), which was supplied with temperature-controlled humidified gases.

The PEFC performance was evaluated at cell temperatures of 90–110 °C and back pressures of 0.3–0.1 MPa and different gas humidification temperatures of 90–59 °C. The gas flow was controlled to keep constant utilization of H_2 at 60, 70 or 80% and of air at 15, 30 or 50%, depending on the humidification condition. The cell resistance (R_c) and electrode reaction resistance (R_{el}) were determined by the AC impedance cole–cole plots. The *through-plane* proton conductivity under PEFC operation ($\sigma_{\perp,FC}$) was evaluated by assuming that the membrane resistance is approximately equal to the cell resistance.

Hydrogen crossover across a membrane was measured by linear sweep voltammetry at a cell temperature of 90 °C, an anode/cathode gas humidification temperature of 85/85 °C (82% RH) and a back pressure of 0.2 MPa. The potential of the cathode (in N_2) was swept at 0.5 mV s^{-1} from 50 to 500 mV vs. reference. Hydrogen crossover was evaluated as the diffusion-limited hydrogen oxidation current obtained in the range of 300–400 mV vs. reference.

3. Results and discussion

3.1. Physicochemical properties

Table 1 lists the physicochemical properties of uncrosslinked SPI membranes (M1 and M2) and their crosslinked membranes (MX1 and MX2) together with those of Nafion NR212 membrane. The crosslinked SPI membranes became insoluble in *m*-cresol containing TEA, whereas the precursor membranes were soluble. The membrane thickness was in the range of 34–48 μm. MX1 and MX2 had a little smaller IECs and water uptakes than M1 and M2, respectively, and as a result had a little smaller proton conductivities. Compared to MX1, MX2 had a little larger water uptake and a little larger proton conductivity as a result of 10% larger IEC. The IEC, water uptake and proton conductivity were in the order, M2 > MX2 > M1 > MX1. Both MX1 and MX2 showed anisotropic membrane swelling with about 10 times larger dimensional changes in the thickness direction than in the plane one. They also showed the anisotropic proton conductivity with about 30% smaller *through-plane* conductivity than *in-plane* one. The

Table 1
Physicochemical properties of SPI and Nafion NR212 membranes.

Code	NTDA-based SPIs	IEC[a] (mequiv g^{-1})	WU[b] (%)	Size change[b]		$\sigma_{//}$[c] (mS/cm)			$\sigma_{\perp}$[d] (mS/cm)		$\sigma_{\perp}/\sigma_{//}$	M[e] (GPa)	S[f] (MPa)	E[g] (%)
				Δt_c	Δl_c	30	50	70	Water	Water				
M1	BSPOB/BAPBz(2/1)	(1.96)1.86	76	0.47	0.039	0.6	8.6	33	165	116	0.70	2.6	139	62
M2	BSPOB/BAPBz(3/1)	(2.08)2.02	90	0.52	0.062	1.6	12	45	185					
MX1	BSPOB/BAPBz(2/1)-XSO_2	1.73	72	0.43	0.050	0.6	6.1	27	148	107	0.72	2.2	102	19
MX2	BSPOB/BAPBz(3/1)-XSO_2	1.95	87	0.53	0.059	1.1	9.3	37	175	130	0.74	2.3	105	26
Nafion NR212		(0.91)0.89	39	0.14	0.13	9.8	30	59	141	136	0.98	0.2	37	410

[a] By titration method, data in parentheses are the calculated one.
[b] At 30 °C.
[c] Proton conductivity at 30% RH, 50% RH, 70% RH and in water at 60 °C.
[d] In water at 60 °C.
[e] Young's modulus.
[f] Stress at break.
[g] Elongation at break.

anisotropy degrees of membrane swelling and proton conductivity for the crosslinked membranes were similar to those for the uncrosslinked ones [23]. They had sufficiently high mechanical strength and toughness.

Fig. 2 shows the relative humidity (RH) dependence of *in-plane* proton conductivity ($\sigma_{//}$) at 60 °C. The SPI membranes displayed larger humidity dependence of conductivity than NR212. For example, the $\sigma_{//}$ values at 50% and 30% RH for M1 were about a tenth and a hundredth, respectively, of that (65 mS cm^{-1}) at 80% RH, whereas the corresponding $\sigma_{//}$ values for NR212 were about three tenths and a tenth, respectively, of that (85 mS cm^{-1}) at 80% RH.

3.2. PEFC performance at 90 °C

Fig. 3(a)–(c) shows the effects of pressure and gas humidity on PEFC performance for M1 at a cell temperature of 90 °C. Anode/cathode gas humidification temperatures were set at 85/80, 72/72 and 59/59 °C, which corresponded to 82/68%, 48/48% and 27/27% RH, respectively (here after abbreviated to 82/68% RH, 48% RH and 27% RH). Table 2 lists the PEFC performance data of open-circuit voltage (OCV), cell voltage at 0.5 A cm^{-2} ($V_{0.5}$), maximum output (W_{max}), the *through-plane* proton conductivity ($\sigma_{\perp,FC}$) and electrode reaction resistance (R_{el}). At a high pressure of 0.3 MPa, with decreasing the humidity from 82/68% RH to 27% RH, the cell performance decreased slightly as shown in Fig. 3(a); that is, $V_{0.5}$ became from 0.75 to 0.74 V and W_{max} became from above 0.93 W cm^{-2} to 0.85 W cm^{-2}. At 82/68% RH, with decreasing the pressure from 0.3 to 0.15 MPa, the cell performance also decreased slightly (see the triangle keys in Fig. 3(a)–(c)); that is, $V_{0.5}$ and W_{max} were 0.71 V and 0.78 W cm^{-2}, respectively, at 0.15 MPa. At 0.2 MPa, as shown in Fig. 3(b), the cell performance decreased fairly with decreasing the humidity, but was still kept in a relatively high level even at 27% RH, namely, $V_{0.5}$ of 0.68 V and W_{max} of 0.51 W cm^{-2}. At 0.15 MPa, as shown in Fig. 3(c), the cell performance decreased largely with decreasing the humidity. The cell performance at 27% RH and 0.15 MPa was in a low level, namely, $V_{0.5}$ of 0.42 V and W_{max} of 0.21 W cm^{-2}.

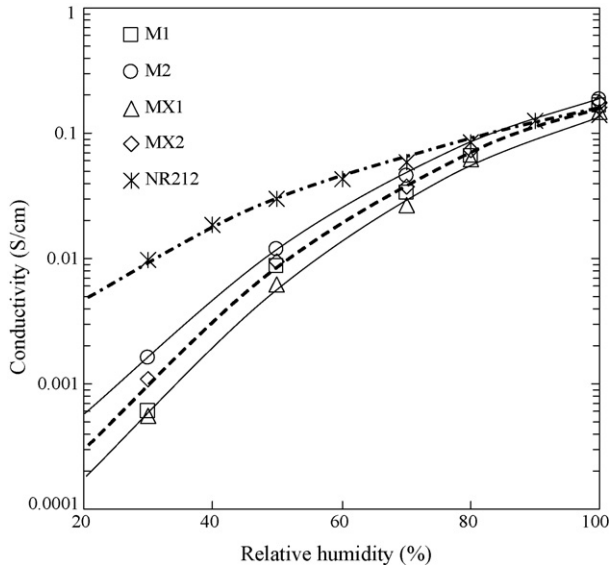

Fig. 2. Relative humidity dependence of proton conductivity ($\sigma_{//}$) of SPI (M1, M2, MX1 and MX2) and Nafion NR212 membranes at 60 °C.

It is noted that the *through-plane* proton conductivity ($\sigma_{\perp,FC}$) under PEFC operation listed in Table 2 reflects the behavior of the cell performance mentioned above. At 82/68% RH, the $\sigma_{\perp,FC}$ for M1 was in the range of 70 mS cm^{-1} (at 0.3 MPa) to 53 mS cm^{-1} (at 0.15 MPa). On the other hand, the *in-plane* proton conductivity ($\sigma_{//}$) at 80% RH and 60 °C was 65 mS cm^{-1} (see Table 1 and Fig. 2). Assuming the activation energy of $\sigma_{//}$ as 10 kJ mol^{-1} and the anisotropy degree of proton conductivity ($\sigma_{\perp}/\sigma_{//}$) as 0.70 [21], the $\sigma_{\perp}$ value at 80% RH and 90 °C was estimated to be about 70 mS cm^{-1}, which was comparable to the $\sigma_{\perp,FC}$ values measured at 82/68% RH and 0.3–0.2 MPa. Judging from the humidity dependence of $\sigma_{//}$ (see Fig. 2), the $\sigma_{\perp}$ values at 48% and 27% RH were evaluated to be about a tenth and a hundredth, respectively, of the $\sigma_{\perp}$ value at 80% RH. With decreasing the humidity from 82/68% RH to 27% RH, the $\sigma_{\perp,FC}$ decreased from 70 to 55 mS cm^{-1} at 0.3 MPa, from 67 to 34 mS cm^{-1} at 0.2 MPa and from 53 to 7 mS cm^{-1} at 0.15 MPa. The decreasing rates were 24, 73 and 93% at 0.3, 0.2 and 0.15 MPa, respectively, which were much larger at the lower pressure but much smaller than the estimated value (99%) of the decreasing rate of $\sigma_{\perp}$. This difference was due to the presence of effective back-diffusion of water formed at the cathode into membrane under PEFC operation; that is, the actual water content in membrane under PEFC operation at a low relative humidity was much higher than that in membrane being in equilibrium with the water vapor in feed gas. Furthermore, these results indicate that the back-diffusion of water was more effective at the higher pressure.

Fig. 4(a)–(c) shows the PEFC performances at 90 °C and 0.2 MPa under different relative humidities of (a) 82/68% RH, (b) 48% RH and (c) 27% RH for M1, MX1, MX2 and NR212. They showed the high cell performances at 82/68% RH. At 48% RH, their cell performances decreased fairly, when compared to 82/68% RH. MX1 showed a fairly low performance, namely, $V_{0.5}$ of 0.60 V and W_{max} of 0.46 W cm^{-2}, whereas M1, MX2 and NR212 kept the relatively high performances (0.67–0.69 V and 0.67–0.75 W cm^{-2}). At 27% RH, the cell performances further decreased largely especially for MX1. MX1 showed a low performance, namely, $V_{0.5}$ of 0.51 V and

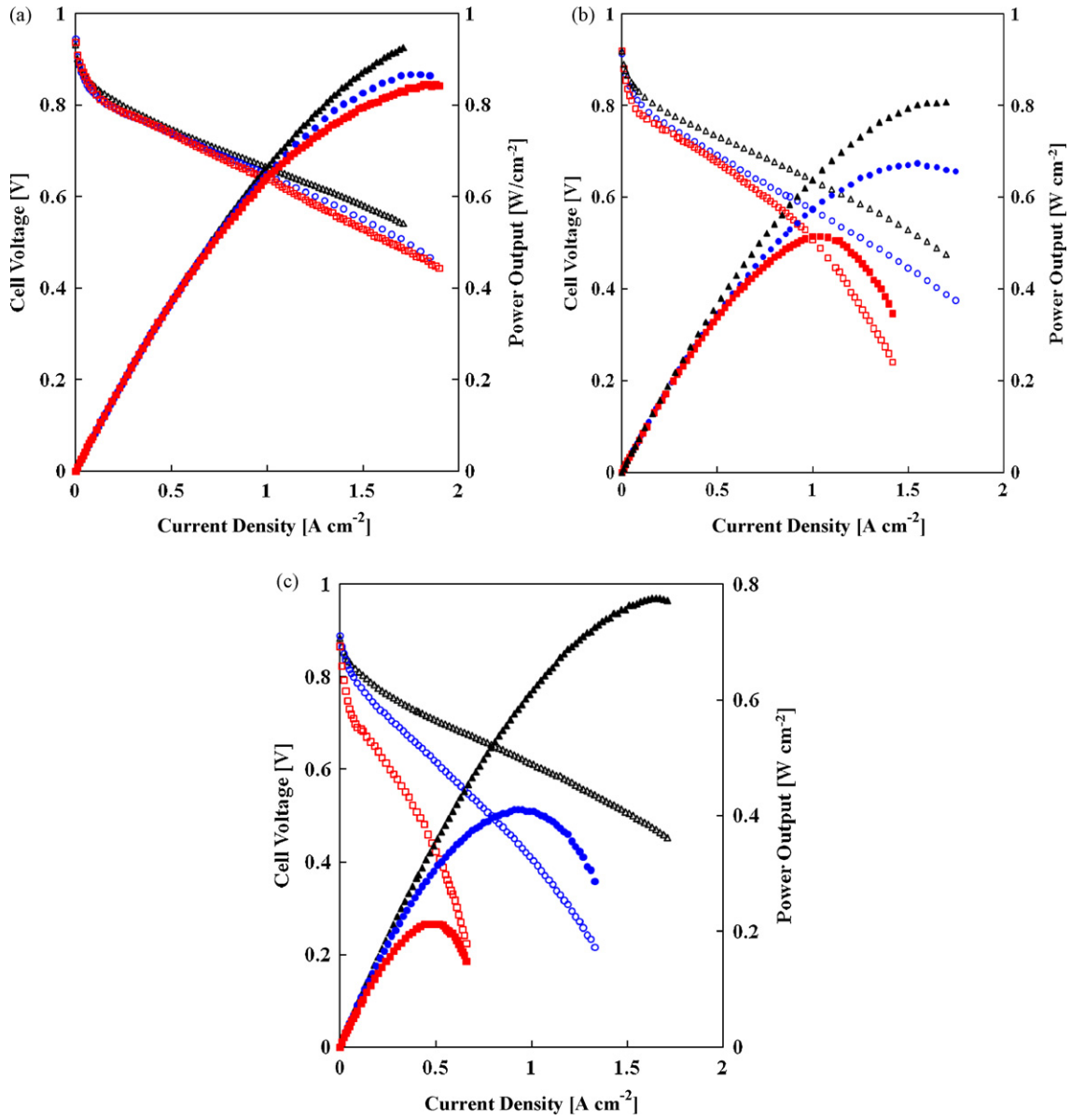

Fig. 3. PEFC performances of M1 membrane at 90 °C and gas pressures of (a) 0.3 MPa, (b) 0.2 MPa and (c) 0.15 MPa under different relative humidities of 82/68% RH (△, ▲), 48% RH (○, ●) and 27% RH (□, ■).

W_{max} of 0.28 W cm^{-2}, whereas the cell performances for M1, MX2 and NR212 were still in the relatively high levels (0.63–0.68 V and 0.51–0.59 W cm^{-2}). MX2 showed the higher cell performance than M1, which was comparable to that of NR212.

It is noted that MX1 with a slightly lower IEC of 1.73 mequiv g^{-1} showed the much lower cell performances at the low relative humidities than M1 and MX2 with slightly higher IECs of 1.86 and 1.95 mequiv g^{-1}, respectively. The $\sigma_{\perp,FC}$ values at 48% and 27% RH of MX1 were 22 and 14 mS cm^{-1}, respectively, which were 40–50% and 60% smaller than those of M1 and MX2 (37–41 and 34–36 mS cm^{-1}). This indicates that the back-diffusion of water was more effective for the SPI membrane with the higher IEC and a small difference in IEC caused a large difference in the wetness of membrane under PEFC operation. It is due to the effective back-diffusion of water in SPI membrane that MX2 showed the comparable PEFC performances to those of NR212 at 48% and 27% RH, in spite of its much lower proton conductivity.

For MX2, the PEFC performance was measured at lower pressures of 0.15 and 0.1 MPa, and the results are shown in Fig. 5. At 82/68% RH, a decrease in pressure from 0.20 to 0.15 MPa hardly affected the cell performance, whereas the decrease from 0.15 to 0.1 MPa largely reduced the performance. However, the cell performance at 0.1 MPa was still kept in a high level, namely, $V_{0.5}$ of 0.62 V and W_{max} of 0.65 W cm^{-2}. On the other hand, at 48% RH, with decreasing the pressure from 0.2 to 0.15 MPa and then to 0.1 MPa, the cell performance was significantly reduced. At 0.1 MPa and 48% RH, MX2 showed a fairly low performance, namely, $V_{0.5}$ of 0.49 V and W_{max} of 0.26 W cm^{-2}.

Fig. 5 also shows the PEFC performances with H_2/O_2 supply at 0.1 MPa, for comparison. The oxygen supply into the cathode significantly enhanced the PEFC performance, compared to the air supply. With the oxygen supply, at 0.1 MPa and 48% RH, MX2 showed a fairly high performance, namely, $V_{0.5}$ of 0.61 V and W_{max} of 0.48 W cm^{-2}. The difference in cell performance between oxygen and air supply were due to the difference in R_{el} rather than that in R_c. In the case of oxygen supply, the R_{el} was smaller in magnitude and its pressure and relative humidity dependence was also smaller, when compared to the air supply. For example, with changing the

Table 2
PEFC performances of SPI (M1, MX1 and MX2) and Nafion NR212 membranes.

Conditions[a]	Code[b]	OCV [V]	$V_{0.5}$ [V]	W_{max} [W cm^{-2}]	$\sigma_{\perp,FC}$[c] [mS cm^{-1}]	R_{el}[c] [mΩ cm^2]
90/0.3/82[d]	M1	0.98	0.75	0.93	70	220
90/0.3/48	M1	1.00	0.74	0.86	62	233
90/0.3/27	M1	0.99	0.74	0.85	55	203
90/0.2/82[d]	M1	0.98	0.73	0.82	67	223
	MX1	0.95	0.66	0.74	40	137
	MX2	0.96	0.68	0.85	49	132
	NR212	0.93	0.69	0.86	90	197
90/0.2/48	M1	0.99	0.69	0.67	37	263
	MX1	0.95	0.60	0.46	22	208
	MX2	0.96	0.67	0.71	43	238
	NR212	0.94	0.68	0.75	70	263
90/0.2/27	M1	0.98	0.68	0.51	34	425
	MX1	0.96	0.51	0.28	14	–
	MX2	0.96	0.63	0.59	37	430
	NR212	0.93	0.66	0.57	58	486
90/0.15/82[d]	M1	0.97	0.71	0.78	53	253
	MX2	0.95	0.70	0.85	68	218
	(MX2)	0.99	0.76	>1.36	70	76
90/0.15/48	M1	0.99	0.62	0.41	17	476
	MX2	0.94	0.58	0.42	21	258
	(MX2)	1.00	0.71	0.99	39	76
90/0.15/27	M1	0.98	0.42	0.21	(7)	–
90/0.1/82[d]	MX2	0.93	0.62	0.65	60	218
	(MX2)	0.98	0.71	>1.18	69	96
90/0.1/48	MX2	0.94	0.49	0.26	(14)	(370)
	(MX2)	0.99	0.61	0.48	19	111
110/0.2/49	M1	0.97	0.30	0.17	(7)	–
	MX1	0.92	0.23	0.14	(6)	–
	MX2	0.95	0.55	0.30	(14)	(570)
110/0.3/49	MX1	0.95	0.55	0.32	13	510
	MX2	0.96	0.69	0.63	38	310
	NR212	0.95	0.70	0.76	78	324
110/0.3/33	M1	0.98	0.45	0.23	(9)	–
	MX1	0.90	0.20	0.16	(5)	–
	MX2	0.97	0.62	0.42	20	602
	NR212	0.95	0.67	0.53	49	486

[a] PEFC operation conditions (x/y/z); x, y and z refer to cell temperature, gas pressure and gas relative humidity, respectively.
[b] (MX2) refers to the case of pure oxygen supply into the cathode, and the others refer to air supply.
[c] At 1 A cm^{-2}; the data in parentheses were measured at 0.5 A cm^{-2}.
[d] Hydrogen/air humidities were 82/68% RH.

pressure and humidity from 0.15 MPa and 82/68% RH to 0.1 MPa and 48% RH, the R_{el} for MX2 changed from 76 to 111 mΩ cm^2 for the oxygen supply, whereas it changed from 218 to 370 mΩ cm^2 for the air supply.

Thus, MX2 showed the high PEFC performances at 90 °C, 0.1 MPa and 82/68% RH. At a low humidity less than 50% RH, a higher pressure above 0.15 MPa was necessary to achieve the reasonably high cell performance. At 48% RH and ambient pressure (0.1 MPa), MX2 showed the fairly low performance with the air supply because of both the larger R_{el} and smaller $\sigma_{\perp,FC}$. On the other hand, with the oxygen supply, the reasonably high performance was maintained at 48% RH and ambient pressure, because of the smaller R_{el} or the smaller resistance of cathode reaction.

3.3. Hydrogen crossover at 90 °C

Hydrogen permeability coefficient (P_{H2}) values were calculated from hydrogen crossover currents and are listed in Table 3 together with the reference data [26–29]. The P_{H2} data are presented in Barrer unit, namely, 1 Barrer = 1×10^{-10} cm^3(STP) cm cm^{-2} s^{-1} cmHg^{-1}. The P_{H2} value for NR212 obtained in this study at 90 °C, 0.2 MPa and

Table 3
Hydrogen permeability coefficients of PEMs evaluated from hydrogen crossover currents.

PEMs	Conditions[a]	P_{H2} [Barrer]	Ref.
M1	90/0.2/82	29	This
MX1		6	
MX2		23	
Nafion NR212		113	
SPI-8[b]	40/0.1/100	14	26
Nafion NR212		35	
SPEEK-51[b]	80/0.1/100	33	27
	80/0.1/66	23	
Nafion 112	80/0.2/100	111	28
	80/0.2/50	89	
	110/0.2/50	115	
Nafion 112	100/0.1/70	94	29

[a] Measurement conditions of hydrogen crossover current: (x/y/z); x, y and z refer to cell temperature, gas pressure and gas relative humidity, respectively.
[b] See the text.

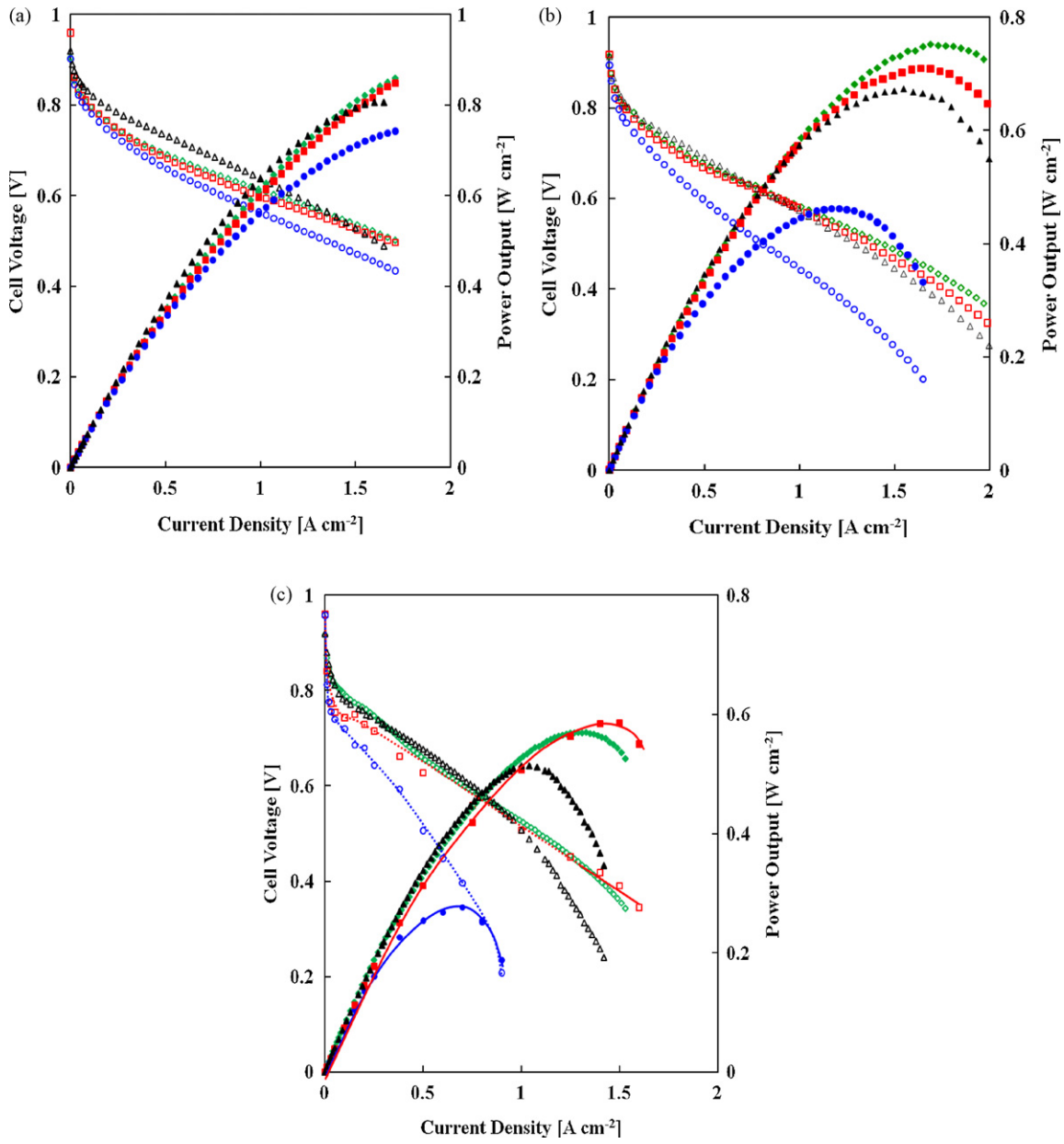

Fig. 4. PEFC performances of M1 (△, ▲), MX1 (○, ●), MX2 (□, ■) and NR212 (◇, ◆) membranes at 90 °C, 0.2 MPa and different relative humidities of (a) 82/68% RH, (b) 48% RH and (c) 27% RH.

82% RH was 113 Barrer, which was reasonable compared to the reported values at different measurement conditions [28,29]. The P_{H2} was in the order, NR212 ≫ MX2, M1 ≫ MX1. MX1 showed a small P_{H2} value of 6 Barrer, which was a quarter of that for M1, indicating that the crosslinking significantly reduced the hydrogen crossover. The P_{H2} values for M1 and MX2 were about four times smaller than that for NR212. Another type of SPI (SPI-8) with an IEC of 2.33 mequiv g^{-1} which were derived from NTDA and sulfonated and nonsulfonated diamines bearing sulfopropoxy pendant groups and triazole groups, respectively, have been reported to have a hydrogen crossover current of 0.2 mA cm^{-2} (corresponding to P_{H2} value of 14 Barrer) at 40 °C, 0.1 MPa and 100% RH [26]. The hydrogen crossover for M1 and MX2 is considered to be slightly lower than that for SPI-8, judging from the comparison with that for NR212, probably because of the lower IECs and to be comparable to that of sulfonated poly(ether ether ketone) (SPEEK) with an IEC of 1.6 mequiv g^{-1} [27].

3.4. PEFC performance at 110 °C

Fig. 6 shows the PEFC performances for M1, MX1 and MX2 at 110 °C, 0.2 MPa and gas humidification temperature of 90 °C (corresponding to 49% RH). The cell voltage largely decreased with increasing load current density, resulting in a low W_{max}. The cell performances at 110 °C for all the membranes were much lower than those at 90 °C shown in Fig. 4(b). For example, the $V_{0.5}$ and W_{max} values at 110 °C and 49% RH for MX2 were 0.55 V and 0.30 W cm^{-2}, respectively, which were 18% and 60% smaller than those at 90 °C and 48% RH. M1 showed the much lower cell performance, namely, $V_{0.5}$ of 0.30 V and W_{max} of 0.17 W cm^{-2}. These were due to the much lower $\sigma_{\perp,FC}$ values at 110 °C. With an increase in cell temperature from 90 to 110 °C, the $\sigma_{\perp,FC}$ values decreased from 36 to 13 mS cm^{-1} for MX2 and 34 to 6.9 mS cm^{-1} for M1. Thus, the cell performance and $\sigma_{\perp,FC}$ decreased more significantly for the SPI membrane with the lower IEC. These results indicate that the back-diffusion of produced water was much less effective at 110 °C,

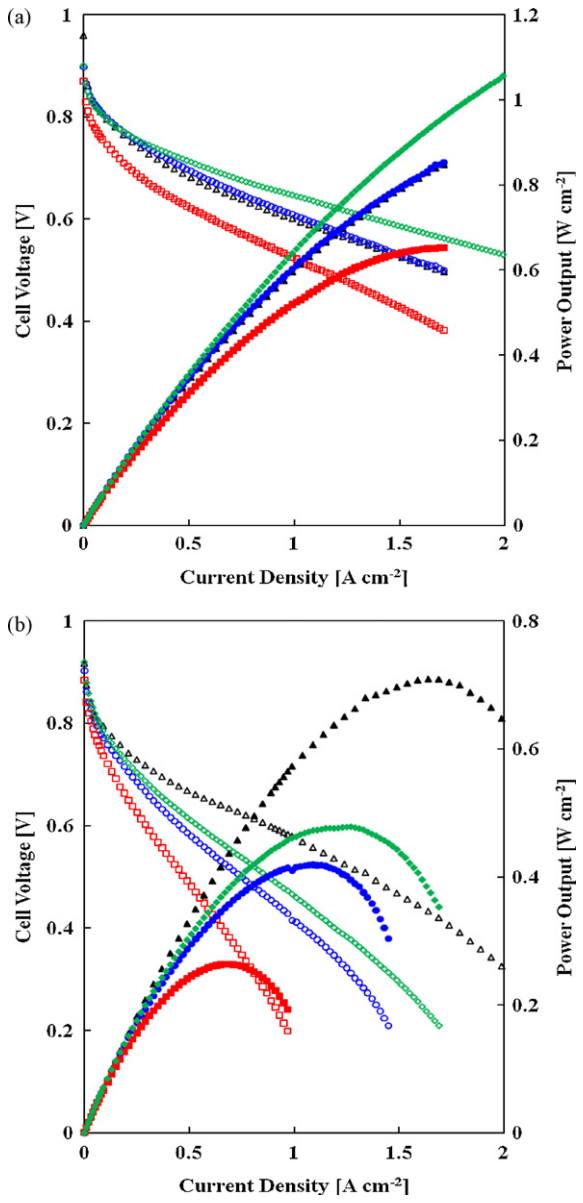

Fig. 5. PEFC performances of MX2 membrane at 90 °C and relative humidities of (a) 82/68% RH and (b) 48% RH at different pressures of 0.2 MPa (△, ▲), 0.15 MPa (○, ●), 0.1 MPa (□, ■) and 0.1 MPa with oxygen supply (◇, ◆).

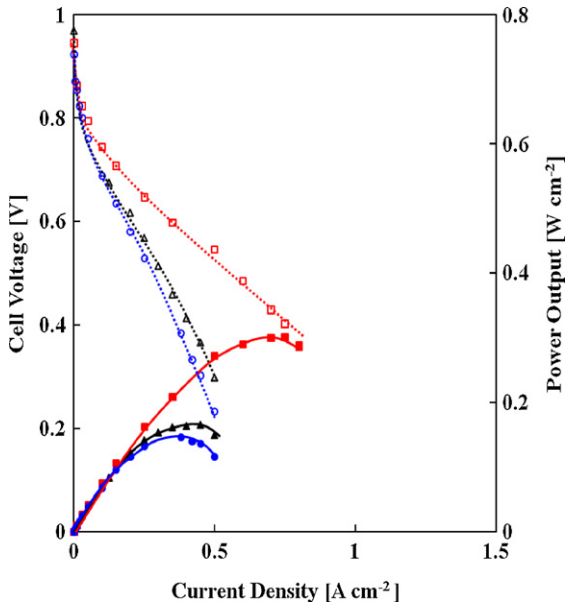

Fig. 6. PEFC performances of M1 (△, ▲), MX1 (○, ●), and MX2 (□, ■) membranes at 110 °C, 0.2 MPa and 49% RH.

when compared to 90 °C, especially for the SPI membrane with the lower IEC.

The PEFC performances were measured for M1, MX1, MX2 and NR212 at 110 °C, a higher pressure of 0.3 MPa and gas humidification temperatures of 90 and 80 °C (corresponding to 49% and 33% RH, respectively). The results are shown in Fig. 7. The cell performance was much improved at 0.3 MPa compared to 0.2 MPa. For MX2, the cell voltage decreased rather slowly with increasing load current density, resulting in the relatively high W_{max} values of 0.56 and 0.42 W cm^{-2} at 49% and 33% RH, respectively, which were 1.8 and 2.6 times larger than those for MX1. It is noted that MX2 with a 10% larger IEC could maintain the PEFC performance at 110 °C and 49–33% RH in a relatively high level due to less reduction in the back-diffusion of produced water. In other words, the higher IEC enhanced the water-holding capacity at the high temperature and the low humidity. The PEFC performances of NR212 were higher than those of MX2. This was due to the much higher proton conductivity at low relative humidity rather than the more effective back-diffusion of water.

The durability test under the open-circuit conditions was carried out for PEFCs with MX2 and NR212 at 110 °C, 0.2 MPa and 49% RH for 1000 h. The results are shown in Fig. 8. For MX2, the OCV decreased gradually from 0.97 V with the elapsed time and then was kept at an almost constant level of 0.81 V after 400 h till 970 h. After 1000 h, the OCV was 0.79 V and the test was stopped. When the cell was open, a break of membrane along the gasket edge was observed. On the other hand, for NR212, the OCV decreased very rapidly with the elapsed time and became 0.2 V after 75 h and 50 h at 49% and 33% RH, respectively. MX2 membrane showed the fairly good durability in PEFC operation at 110 °C and 49% RH, but NR212 showed the very poor durability.

For the short-term durability test, a PEFC with MX2 (43 μm in thickness) was operated under a constant load current density of 0.25 A cm^{-2} at 110 °C, 49% RH and 0.2 MPa for 300 h. The OCV and cell voltage decreased from 0.96 to 0.85 V and from 0.65 to 0.62 V, respectively, and the cell resistance increased from 63 to 75 mΩ after 300 h. Fig. 9 shows the polarization and power output curves for MX2 before and after the durability test. The cell performance at 110 °C, 49% RH and 0.2 MPa became slightly lower after the durability test; for example $V_{0.5}$ and W_{max} values decreased from 0.51 to 0.49 V and from 0.33 to 0.28 W cm^{-2}, respectively. The OCV reduction rate was about 370 μV h^{-1}, which was very high and comparable to that observed in the early stage of the durability test under the open-circuit conditions. The $\sigma_{\perp,FC}$ hardly changed (16–15 mS cm^{-1}) and the R_{el} slightly increased from 480 to 520 mΩ cm^2. The hydrogen crossover currents measured at 90 °C, 0.2 MPa and 82% RH before and after the durability test were 0.7 and 5.0 mA cm^{-2}, respectively. The P_{H2} value increased from 23 to 170 Barrer by the durability test.

In the durability experiments of PEFCs, a decrease in OCV and an increase in hydrogen crossover are generally considered as signs of membrane degradation in PEFC operation [26,30–32]. Inaba et al. reported hydrogen crossover and membrane degradation in PEFCs with perfluoro PEMs under open-circuit conditions at 80 °C and 42% RH [30]. For the first 30 days, the OCV decreased from 0.96 to 0.89 V, whereas the hydrogen crossover current hardly changed at 0.8 mA cm^{-2}. For the second 30 days, the crossover

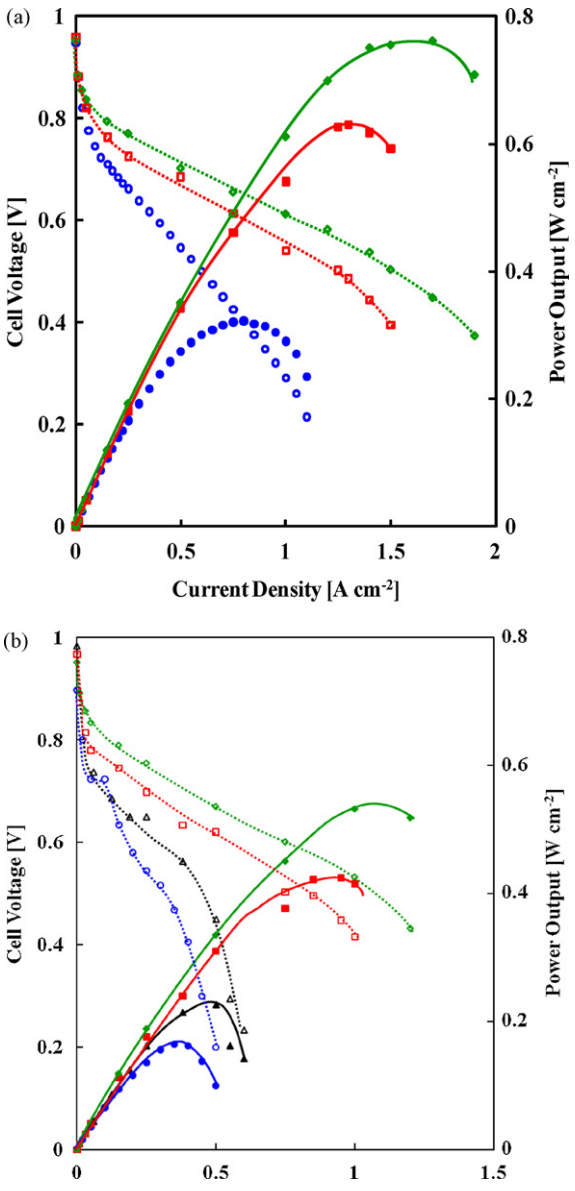

Fig. 7. PEFC performances of M1 (△, ▲), MX1 (○, ●), and MX2 (□, ■) and NR212 (◇, ◆) membranes at 110 °C, 0.3 MPa and relative humidities of (a) 49% RH and (b) 33% RH.

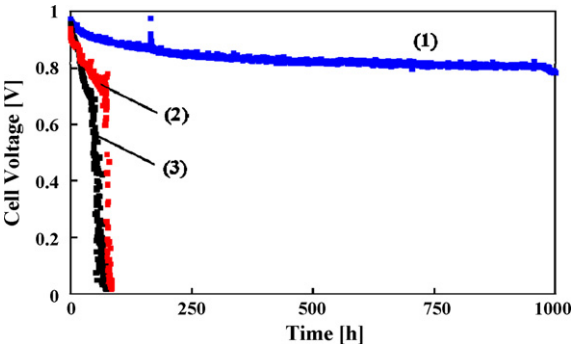

Fig. 8. Variation of OCV of PEFCs with MX2 and NR212 during OCV durability test at 110 °C and 0.2 MPa for 1000 h. (1) MX2 at 49% RH, (2) NR212 at 49% RH and (3) NR212 at 33% RH.

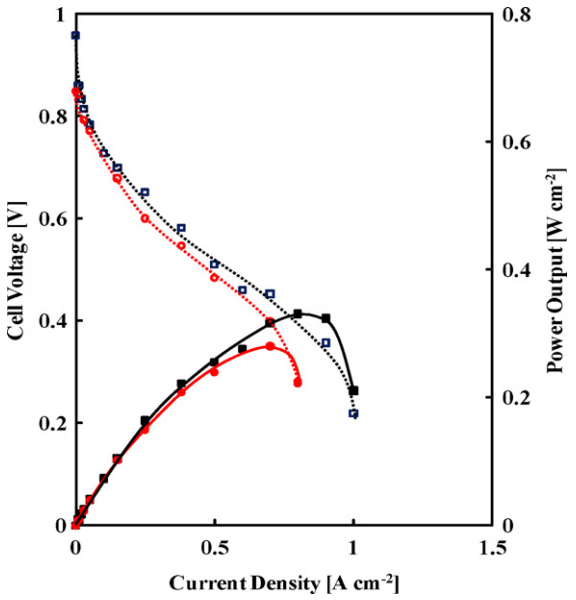

Fig. 9. Performances of PEFC with MX2 at 110 °C, 49% RH and 0.2 MPa before (□,■) and after (○, ●) the short durability test operated under a constant load current density of 0.25 A cm^{-2} at 110 °C, 49% RH and 0.2 MPa for 300 h.

current increased gradually from 0.8 to 11 mA cm^{-2}, which corresponded to a large increase in P_{H2} of 37–510 Barrer, and the OCV decreased from 0.89 to 0.84 V. They attributed the first drop in OCV to the degradation of platinum catalyst and the second drop to fatal damages of membrane. Liu et al. carried out durability study of PEFCs with Nafion 112 under dynamic testing conditions at 80 °C, 0.138 MPa and 100% RH [31] and observed a much larger increase in the crossover current from 10 to 190 mA cm^{-2} (from 600 to about 10,000 Barrer in P_{H2}) with a relatively small drop in OCV of 0.90–0.85 V [31]. The similar large increase in the crossover current was also reported for PEFCs with composite membranes composed of SPEEK and stabilized phosphotungstic acid which were operated at 80 °C and 50–75% RH for 30 h [32]. On the other hand, Watanabe et al. reported on the high durability of PEFCs with SPI-8 mentioned above. After being operated at 80 °C, 0.1 MPa and 100% RH or 100/40% RH for 5000 h, the PEFCs showed no significant decrease in OCV and no increase in crossover current [30]. We also reported on the high durability of PEFCs with MX1 operated at 90 °C, 0.3 MPa and 84–30% RH. The OCV hardly changed during the durability tests for 1600 h or 1000 h.

In the present durability tests at 110 °C, 0.2 MPa and 49%RH, PEFCs with MX2 showed the relatively large drop in OCV from 0.96 to 0.85 V in the early stage till 300 h, with keeping the rather small increase in hydrogen crossover (from 23 to 170 Barrer). This is different from the cases of Nafion 112, perfluoro PEM and SPEEK composite membranes mentioned above [30–32]. The similar large drop in OCV has been reported for the aromatic PEM based on sulfonated poly(*p*-phenylene) at 110 °C and 50% RH, in spite of its excellent durability at temperatures of 95 °C to −20 °C [12]. The OCV drop at high temperature of 110 °C might be related with some degradation of the platinum catalyst.

4. Conclusions

PEFC performance of crosslinked BSPOB-based SPI membranes was largely affected by the operation conditions of temperature, pressure and relative humidity. At 90 °C and relatively high humidification of 82/68% RH, the cell performance was hardly affected by the pressure and was kept in a high level even at 0.1 MPa. At low humidification of 48% and 27% RH, the cell performance was still

kept in a reasonably high level at high pressures above 0.2 MPa, but it largely decreased at low pressures below 0.15 MPa. A slight decrease in IEC of membrane caused a relatively large decrease in the cell performance at a low relative humidity. With an increase in temperature from 90 to 110 °C, the cell performance largely decreased. For example, the W_{max} for MX2 was 0.30 W cm^{-2} at 110 °C, 0.2 MPa and 49% RH, which was less than a half of the corresponding value (0.71 W cm^{-2}) at 90 °C. These results indicate that the back-diffusion of water formed at cathode into membrane became less effective at the lower pressure and the higher temperature and for membrane with the lower IEC, resulting in the larger decrease in *through-plane* proton conductivity under PEFC operation. At 110 °C, 0.3 MPa and 49% RH, MX2 with a higher IEC of 1.9 mequiv g^{-1} showed the fairly high performance, namely, $V_{0.5}$ of 0.69 V and W_{max} of 0.63 W cm^{-2}, and the fairly good durability in PEFC operation and OCV conditions.

To achieve the high cell performance at relatively high temperatures of 100–120 °C and low relative humidities of 50–20% RH and low pressures of 0.15–0.1 MPa, it is essentially required to develop higher performance PEMs with the higher *through-plane* conductivity at the low relative humidities. Hybrid membranes doped with hydrophilic and proton-conductive inorganic porous fillers might be useful as high temperature PEMs due to the promoted effect of the back-diffusion of water.

Acknowledgements

This work was financially supported by the New Energy and Industrial Technology Development Organization (NEDO) and by a Grand-in-aid for Development Science Research (No. 19550209) from the Ministry of Education, Science and Culture of Japan.

References

[1] O. Savadogo, J. New Mater. Electrochem. Syst. 1 (1998) 47–66.
[2] K.A. Mauritz, R.B. Moore, Chem. Rev. 104 (2004) 4535–4586.
[3] R. Souzy, B. Ameduri, Prog. Polym. Sci. 30 (2005) 644–687.
[4] M. Rikukawa, K. Sanui, Prog. Polym. Sci. 25 (2000) 1463–1502.
[5] J.A. Kerres, J. Membr. Sci. 185 (2001) 3–27.
[6] K.D. Kreuer, J. Membr. Sci. 185 (2001) 29–39.
[7] Q. Li, R. He, J.O. Jensen, N. Bjerrum, Chem. Mater. 15 (2003) 4896–4915.
[8] M.A. Hickner, H. Ghassemi, Y.S. Kim, B.R. Einsla, J.E. McGrath, Chem. Rev. 145 (2004) 4587–4612.
[9] W.L. Harrison, M.A. Hickner, Y.S. Kim, J.E. McGrath, Fuel Cells 5 (2005) 201–212.
[10] Y. Yin, O. Yamada, K. Tanaka, K. Okamoto, Polym. J. 38 (2006) 197–219.
[11] C. Marestin, G. Gebel, O. Diat, R. Mercier, Adv. Polym. Sci. 216 (2008) 185–258.
[12] K. Goto, I. Rozhanskii, Y. Yamakawa, T. Otsuki, Y. Naito, Polym. J. 41 (2009) 95–105.
[13] J.M. Bae, I. Honma, M. Murata, T. Yamamoto, M. Rikukawa, N. Ogata, Solid State Ionics 147 (2002) 189–194.
[14] T. Yamaguchi, H. Zhou, S. Nakazawa, N. Hara, Adv. Mater. 19 (2007) 592–596.
[15] N. Asano, M. Aoki, S. Suzuki, K. Miyatake, H. Uchida, M. Watanabe, J. Am. Chem. Soc. 128 (2006) 1762–1769.
[16] K. Miyatake, Y. Chikashige, E. Higuchi, M. Watanabe, J. Am. Chem. Soc. 129 (2007) 3879–3887.
[17] A. Roy, H.S. Lee, J.E. McGrath, Polymer 49 (2008) 5037–5044.
[18] M.L. Einsla, Y.S. Kim, M. Hawley, H.S. Lee, J.E. McGrath, B. Liu, M.D. Guiver, B.S. Pivovar, Chem. Mater. 20 (2008) 5636–5642.
[19] H. Bai, W.S. Winston Ho, J. Membr. Sci. 313 (2008) 75–85.
[20] C.H. Lee, C.H. Park, Y.M. Lee, J. Membr. Sci. 313 (2008) 199–206.
[21] Y. Sutou, Y. Yin, Z. Hu, S. Chen, H. Kita, K. Okamoto, H. Wang, H. Kawasato, J. Polym. Sci. Part A: Polym. Chem. 47 (2009) 1463–1477.
[22] N. Endo, K. Matsuda, K. Yaguchi, Z. Hu, K. Chen, M. Higa, K. Okamoto, J. Electrochem. Soc. 156 (2009) B628–B633.
[23] Z. Hu, Y. Yin, K. Yaguchi, N. Endo, M. Higa, K. Okamoto, Polymer 50 (2009) 2933–2943.
[24] M. Kido, Z. Hu, T. Ogo, Y. Sutou, K. Okamoto, J. Fang, Chem. Lett. 36 (2007) 272–273.
[25] J. Fang, F. Zhai, X. Guo, H. Xu, K. Okamoto, J. Mater. Chem. 17 (2007) 1102–1108.
[26] A. Kabasawa, J. Saito, H. Yano, K. Miyatake, H. Uchida, M. Watanabe, Electrochim. Acta 54 (2009) 1076–1082.
[27] R. Jiang, H.R. Kunz, J.M. Fenton, J. Power Sources 150 (2005) 120–128.
[28] X. Cheng, J. Zhang, Y. Tang, C. Song, J. Shen, D. Song, J. Zhang, J. Power Sources 167 (2007) 25–31.
[29] Y. Song, J.M. Fenton, H.R. Kunz, L.J. Bonville, M.V. Williams, J. Electrochem. Soc. 152 (2005) A539–544.
[30] M. Inaba, T. Kinumoto, M. Kiriaki, R. Umebayashi, A. Tasaka, Z. Ogumi, Electrochim. Acta 51 (2008) 5746–5753.
[31] D. Liu, S. Case, J. Power Sources 162 (2006) 521–531.
[32] V. Ramani, S. Swier, M.T. Shaw, R.A. Weiss, H.R. Kunz, J.M. Fenton, J. Electrochem. Soc. 155 (2008) B532–B537.